Controlling synchronization in a complex network of nonlinear oscillators via feedback linearisation and H_-control

# Controlling synchronization in a complex network of nonlinear oscillators via feedback linearisation and $\mathcal{H}_\infty$-control

Nicolás Faedo[a,*], Demián García-Violini[b], John V. Ringwood[a]

[a] *Deparment of Electronic Engineering, Maynooth University, Co. Kildare, Ireland*
[b] *Departamento de Ciencia y Tecnología, Universidad Nacional de Quilmes, Bernal, Argentina*

**Abstract**

This short communication proposes a strategy to induce complete synchronization in a complex network composed of a general class of nonlinear dynamical oscillators. To that end, we formulate complete synchronization as a robust stabilisation problem, and propose a multiple-input multiple-output feedback decoupling linearisation algorithm in combination with $\mathcal{H}_\infty$-control, designed to achieve a stable synchronization even in the presence of model uncertainty. We illustrate the strategy via a case study, where a complex network composed of FitzHugh-Nagumo oscillators is considered.

*Keywords:* Complex networks, Oscillators, Feedback linearisation, Robust control, Synchronization, Consensus

## 1. Introduction

Coupled dynamical systems are ubiquitous in nature and science, and have been the focus of substantial research within the nonlinear systems community, specifically from scientists specialising in the field of *complex networks* [1]. A particularly relevant 'family' of network-coupled nonlinear systems, which has attracted a great deal of attention in the past decade, are complex networks of nonlinear oscillators (see, for instance, [2]). Nonlinear oscillators play a fundamental role in characterising and modelling an extensive variety of physical processes, ranging from the fields of power electronics [3] and energy conversion [4], to neuroscience [5] and physiology [6].

Within the research field of coupled nonlinear systems, the problem of *synchronization* appears recursively: Since the seminal study [7], which formalises and characterises so-called *chaos* synchronization, the feasibility of synchronizing network-coupled systems has attracted the wider research community. As a consequence, a number of techniques exist to analyse existence and stability of synchronization regimes/manifolds in coupled systems, including, for instance, networks of periodically oscillating nodes, and chaotic oscillators. These studies include, for example, [8, 9, 10], and analyse conditions on the coupling between network nodes such that synchronization occurs.

Motivated by the inherent relevance of synchronization in a wide range of physical phenomena, researchers from the control community recently started to bring mathematical tools from control theory capable of *externally* achieving different states of synchronization [11], by means of an appropriate *external (user-supplied) control input*[1]. To date, a number of control techniques have been presented in the literature concerning synchronization of coupled oscillators (see, for instance, [12, 13, 14, 15]), which intrinsically depend both upon the network configuration (*i.e.* topology), and the specific synchronization objective. Commonly, these techniques relate to a single specific application study, hindering the scope of application of the proposed methods for a general class of network-coupled systems, hence limiting any results/conclusions to the specific case study presented. A step towards a 'general' framework for *complete* synchronization has been taken in [16], via a model-matching approach. Nonetheless, [16] inherently requires *perfect* knowledge of the dynamics of the network, which is virtually always unavailable in a realistic scenario, where unmodelled dynamics are ubiquitous.

This short communication presents a framework to control *complete synchronization* for a general class of network-coupled nonlinear oscillators, under mild assumptions. To this end, we propose a multiple-input multiple-output feedback decoupling linearisation algorithm in combination with $\mathcal{H}_\infty$-control theory, specifically designed to achieve a robust stable synchronization. The proposed technique is illustrated via a case study, where complete synchronization of a complex network of FitzHugh-Nagumo neurons in external electrical stimulation [17, 18] is addressed.

The remainder of this short communication is organised as follows. Section 1.1 describes the notation utilised throughout this manuscript, while Section 2 formally introduces the problem of complete synchronization from a control perspective. Section 3 proposes a feedback decou-

*Corresponding author
*Email address:* nicolas.faedo@mu.ie (Nicolás Faedo)

[1] Note that this is effectively different from references [8, 9, 10], where the (internal) coupling dynamics are considered to provide conditions on synchronization.

pling strategy capable of achieving linear error dynamics, while Section 4 outlines the proposed robust controller. Finally, Section 5 presents a case study, while Section 6 encompasses the main conclusions of this study.

### 1.1. Notation and conventions

$\mathbb{R}^+$ ($\mathbb{R}^-$) denotes the set of non-negative (non-positive) real numbers. The symbol 0 stands for any zero element, dimensioned according to the context. The notation $\mathbb{N}_q$ indicates the set of all positive natural numbers up to $q$, *i.e.* $\mathbb{N}_q = \{1, 2, \dots, q\}$. The symbol $\mathbb{I}_n$ denotes the identity element of the space of matrices $\mathbb{C}^{n\times n}$. The spectrum of a matrix $A \in \mathbb{R}^{n\times n}$, *i.e.* the set of its eigenvalues, is denoted by $\lambda(A)$. The superscript $\mathsf{T}$ denotes the transposition operator. Let $v$ be an element of a vector space $\mathscr{V}$ defined over a field $K$. The notation $\|v\|$ denotes any norm of $v \in \mathscr{V}$, where the specific norm is always clear from the context. $\mathcal{H}_\infty$ denotes the space of complex-valued functions $F(s)$, $s \in \mathbb{C}$, which are analytic and bounded in the open right half-plane, while $\mathcal{RH}_\infty \subset \mathcal{H}_\infty$ denotes the subspace of rational functions in $\mathcal{H}_\infty$. The mapping $\bar{\sigma} : \mathbb{C}^{n\times m} \to \mathbb{R}^+$ denotes the maximum singular value operator. The *Kronecker product* between $M_1 \in \mathbb{R}^{n\times m}$ and $M_2 \in \mathbb{R}^{p\times q}$ is denoted by $M_1 \otimes M_2 \in \mathbb{R}^{np\times mq}$.

## 2. Preliminaries and problem statement

From now on, we consider a complex network composed of $N$ coupled oscillators, commonly termed *nodes*, where each node is described by a nonlinear dynamical system $\Sigma$ defined over an $n$-dimensional state-space. We make this statement precise in the following. Let each node $i$, with $i \in \mathbb{N}_N$, be defined in terms of a continuous-time, finite-dimensional, single-input system $\Sigma_i$, described, for $t \in \mathbb{R}^+$, by the set of nonlinear differential equations[2]

$$\Sigma_i : \dot{x}_i = Ax_i + Bg(x_i)(u_i + f_i(x_i, \mathbf{x})), \qquad (1)$$

where $x_i(t) \in \mathbb{R}^n$, $A \in \mathbb{R}^{n\times n}$, $B \in \mathbb{R}^n$, and the pair $(A, B)$ is assumed to be controllable. The notation $u_i : \mathbb{R}^+ \to \mathbb{R}$, $t \mapsto u_i(t)$, indicates the external control input acting on the $i$-th node. The network state-vector $\mathbf{x}(t) \in \mathbb{R}^{nN}$ is defined as $\mathbf{x}(t) = [x_1(t), \dots, x_N(t)]$. The nonlinear mappings $g : D_x \to \mathbb{R}$ and $f_i : D_x \times D_\mathbf{x} \to \mathbb{R}$, with $D_x \subset \mathbb{R}^n$ and $D_\mathbf{x} \subset \mathbb{R}^{nN}$, are assumed to be sufficiently smooth, with $g(x_i)$ nonsingular for every $x_i(t) \in D_x$.

*Remark* 1. The nonlinear mapping $f_i$ accounts both for internal, and *coupling*, dynamics, affecting each node comprising the complex network. Note that we do not make any assumption with respect to the coupling directionality.

*Remark* 2. Each node comprising the network, *i.e.* system (1), is assumed to be written in so-called *normal form.* This structure is motivated by the fact that a large number of well-known relevant systems/oscillators can be either written in terms of (1) directly, or via a suitable diffeomorphism [19], *i.e.* a nonlinear change of coordinates. This includes, for instance, Van der Pol and Duffing oscillators, Chua's circuit, Rössler's system, Lorentz's system, and the FitzHugh-Nagumo neuronal model.

Before going any further, we write (1) using a more convenient notation, as

$$\Sigma_i : \dot{x}_i = Ax_i + Bg_{f_i}(x_i, \mathbf{x}) + Bg(x_i)u_i, \qquad (2)$$

where $g_{f_i}(x_i, \mathbf{x}) = g(x_i)f_i(x_i, \mathbf{x})$. We discuss the notion of complete synchronization in the following paragraphs.

The problem of *complete synchronization* [11] consists of the synchronization of the state-vector of a set of nodes, commonly called *slave nodes* (or simply *slaves*), to the dynamics of a set of *leader* or *master* nodes[3]. This problem is also commonly referred in the literature as *consensus with a leader* (see, for instance, [20]). Throughout this communication, we assume a network composed of a single master node, *i.e.* the remainder $N-1$ nodes are slaves, aiming to simplify the notation involved. Note that the extension of the proposed framework to multiple master nodes can be done straightforwardly. In particular, and without any loss of generality, we define node 1 as *leader*, *i.e.* $\Sigma_1 \equiv \Sigma_l$, so that equation (2) can be re-written as,

$$\begin{aligned} \Sigma_l &: \dot{x}_l = Ax_l + Bg_{f_l}(x_l, \mathbf{x}), \\ \Sigma_{\underline{i}} &: \dot{x}_{\underline{i}} = Ax_{\underline{i}} + Bg_{f_{\underline{i}}}(x_{\underline{i}}, \mathbf{x}) + Bg(x_{\underline{i}})u_{\underline{i}}, \end{aligned} \qquad (3)$$

for $\underline{i} \in \{2, \dots, N\} \subset \mathbb{N}$.

*Remark* 3. We assume that the leader node $\Sigma_l$ is not necessarily accessible, *i.e.* $u_1 \equiv u_l = 0$, $\forall t$. In other words, we cannot affect the dynamical behaviour of the master node directly. This scenario, which is inherently more complex that its accessible counterpart, is a natural setting in many practical applications [2].

Using the structure posed in (3), the problem of inducing complete synchronization can be now stated, from a control perspective, as follows. Let $e_{\underline{i}} = x_l - x_{\underline{i}}$, $e_{\underline{i}}(t) \in \mathbb{R}^n$, be the *synchronization error* associated with node $\underline{i}$. Design the control input $u_{\underline{i}} : \mathbb{R}^+ \to \mathbb{R}$, $t \mapsto u_{\underline{i}}(t)$, such that

$$\lim_{t\to+\infty} \|x_l - x_{\underline{i}}\| = \lim_{t\to+\infty} \|e_{\underline{i}}\| = 0, \qquad (4)$$

for all $\underline{i} \in \{2, \dots, N\} \subset \mathbb{N}$, and any norm in $\mathbb{R}^n$.

*Remark* 4. Condition (4) can be alternatively seen from a dynamical 'viewpoint': complete synchronization can be achieved as long as the zero equilibrium of system $\mathcal{E}_i : \dot{e}_{\underline{i}} = \dot{x}_l - \dot{x}_{\underline{i}}$ is asymptotically stable $\forall \underline{i}$.

[2]From now on, the dependence on $t$ is dropped when clear from the context.

[3]Note that the terminology 'master-slave' is commonly used for networks with *directed* coupling, and that complete synchronization can equally occur in networks with mutually coupled nodes. Also note that we use the term 'master' and 'leader' interchangeably.

## 3. Feedback linearisation

Following Remark 4, the objective is to propose a general framework capable of computing a control law $u_{\underline{i}}$ such that the zero equilibrium of the synchronization error system $\mathcal{E}_i$ has strong stability properties. To achieve this, we take two different 'steps', *i.e.* we decompose our control strategy into two parts. The first step towards complete synchronization, proposed in this communication, is based on the concept of feedback linearisation [19]. To make this precise, note that the error system $\mathcal{E}_i$ can be written as

$$\dot{e}_{\underline{i}} = Ae_{\underline{i}} + B\left(g_{f_l}(x_l, \mathbf{x}) - g_{f_{\underline{i}}}(x_{\underline{i}}, \mathbf{x})\right) - Bg(x_{\underline{i}})u_{\underline{i}}. \quad (5)$$

Based on the dynamical equation (5), we now propose $u_{\underline{i}} : \mathbb{R}^+ \to \mathbb{R}$ to be defined as

$$u_{\underline{i}} = g^{-1}(x_{\underline{i}})\left(g_{f_l}(x_l, \mathbf{x}) - g_{f_{\underline{i}}}(x_{\underline{i}}, \mathbf{x}) - \nu_{\underline{i}}\right), \quad (6)$$

where $\nu_{\underline{i}} : \mathbb{R}^+ \to \mathbb{R}$, $t \mapsto \nu_{\underline{i}}(t)$. Note that the inverse mapping $g^{-1}$ is always well-defined by assumption (see Section 2). With the proposed controller $u_{\underline{i}}$ (6), the synchronization error system (5) can be written, in closed-loop, as

$$\mathcal{E}_i : \dot{e}_{\underline{i}} = Ae_{\underline{i}} + B\nu_{\underline{i}}, \quad (7)$$

where $\mathcal{E}_i$ is linear in $e_{\underline{i}}$, with external input $\nu_{\underline{i}}$. Note that (7) is completely decoupled from the network dynamics.

*Remark* 5. The input $\nu_{\underline{i}}$ provides an additional degree-of-freedom, which is used in this communication to achieve complete synchronization in a robust sense. This is specifically discussed in Section 4.

*Remark* 6. System (7) is controllable. The latter property is a direct consequence of the controllability associated with the Jacobian linearisation of system (1) about the zero equilibrium.

Following equation (7), let the network synchronization error state-vector $\mathbf{e} : \mathbb{R}^+ \to \mathbb{R}^{n(N-1)}$ be written as $\mathbf{e}(t) = [e_2(t), \ldots, e_N(t)]$, and let $\mathbf{v}(t) = [\nu_2(t), \ldots, \nu_N(t)] \in \mathbb{R}^{N-1}$. Applying the control law proposed in (6) to each slave node, the closed-loop complex network can be compactly written as

$$\mathcal{E} : \dot{\mathbf{e}} = (\mathbb{I}_{N-1} \otimes A)\,\mathbf{e} + (\mathbb{I}_{N-1} \otimes B)\,\mathbf{v}, \quad (8)$$

where $\mathbf{v}$ is to be designed such as system $\mathcal{E}$ has strong stability properties. This is specifically addressed in Section 4, using a robust $\mathcal{H}_\infty$-approach.

## 4. Robust synchronization

Following the feedback linearisation procedure described in Section 3, we now propose a *robust* controller $\mathcal{K}_\infty(s) \in \mathcal{RH}_\infty$ such that (8) has strong stability properties.

*Remark* 7. The selection of a robust control technique can be direcly motivated as follows: the feedback linearisation procedure, described in Section 3, depends upon precise knowledge of the network dynamics (3), which is not necessarily available in a realistic scenario. To overcome this issue, arising due to the potentially 'inexact' feedback linearisation via (6), the linearised error system (8) is assumed to be *uncertain*. This uncertainty is formally introduced in the following paragraphs.

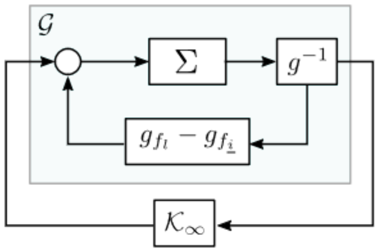


Figure 1: Schematic illustration of the closed-loop system for complete synchronization.

To be precise, we propose the design and synthesis of[4] $\mathcal{K}_\infty$ following robust control theory, particularly based upon the results presented in [21] and [22], for linear time invariant (LTI) $\mathcal{H}_\infty$-control synthesis with pole placement. The closed-loop system (8) is schematically illustrated, from a traditional robust control perspective, in Figure 1, where the nonlinear system $\Sigma$ (representing the full network dynamics), the feedback linearisation path, and the feedback controller $\mathcal{K}_\infty$, are explicitly shown.

Following Remark 7, the control approach considered in this section prioritises the robust stabilisation of (8), while performance specifications are addressed using a set of additional constraints within an LMI-based optimisation problem, following [22]. In particular, the control problem is solved via 'standard' $\mathcal{H}_\infty$-design, guaranteeing robust stability of system (8), while the closed-loop transient response (*i.e.* performance) is addressed by adding a set of LMI constraints for closed-loop pole clustering.

*Remark* 8. The robust control design problem, as addressed in this short communication, is significantly simpler than a standard mixed-sensitivity problem, in which a set of weighting functions is used to handle both nominal and robust performance. This practice increases both the order of the designed system, and the number of singular values involved in the corresponding optimisation procedure. In contrast, the design approach presented in this section seeks to reduce design complexity, while also increasing the stability margin of the closed-loop system [22].

Within this framework, the system in (8), describing the linearised dynamics of the synchronization error, can be generalised in terms of a family of models $\mathcal{G}$, by means of an *unstructured uncertainty* set $\mathbf{\Delta} \subset \mathcal{H}_\infty$, defined as:

$$\mathbf{\Delta} = \{\Delta(s) \in \mathcal{H}_\infty : \|\Delta(s)\|_\infty < 1\}. \quad (9)$$

Let $G_0(s) = (s\mathbb{I}_{n(N-1)} - (\mathbb{I}_{N-1} \otimes A))^{-1}(\mathbb{I}_{N-1} \otimes B)$ be the nominal (LTI) error system. In particular, using a

[4] From now on, we drop the dependence on $s$ when clear from the context.

multiplicative uncertainty scheme, the family of models $\mathcal{G}$ can be expressed as:

$$\mathcal{G} = \left\{ \left(I + \Delta(s) W_\Delta(s)\right) G_0(s),\ \Delta(s) \in \mathbf{\Delta} \right\}, \tag{10}$$

where the stable, causal and minimal system $W_\Delta$, with degree $n_\Delta$, is the so-called uncertainty *weight*, which describes the dynamical behaviour of $\Delta$. Note that $W_\Delta$ is always defined such that the inequality $\bar{\sigma}(W_\Delta(\jmath\omega)) > \bar{\sigma}(\Delta(\jmath\omega))$ holds, for all $\omega \in \mathbb{R}$. The expression in equation (10) is schematically depicted in Figure 2, where the disturbance vector is such that $y_\Delta(s) \in \mathbb{C}^{n(N-1)}$.

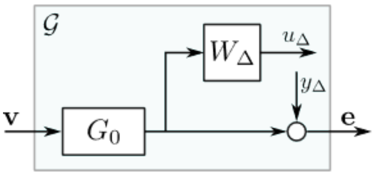


Figure 2: Multiplicative uncertainty structure.

*Remark* 9. The definition of the family of models $\mathcal{G}$ in (10), via $W_\Delta$, can be achieved using different methods, according to the specifics of the complex network (3). This includes both exhaustive numerical simulation, or experimental testing (if available).

Based on the family of models $\mathcal{G}$, we now propose a modification of the classical LMI-based design method for $\mathcal{H}_\infty$-controllers (which arises from the well-known bounded-real lemma [23]), by including a set of LMI-based constraints, aiming to handle the location of the closed-loop eigenvalues [22]. To achieve this objective, the so-called closed-loop linear fractional transformation (LFT) structure:

$$\underbrace{\begin{bmatrix} u_\Delta \\ \mathbf{e} \end{bmatrix}}_{z} = \underbrace{\begin{bmatrix} 0 & W_\Delta(s) \\ I & G_0(s) \end{bmatrix}}_{M} \underbrace{\begin{bmatrix} y_\Delta \\ \mathbf{v} \end{bmatrix}}_{w}. \tag{11}$$

In particular, let the *LFT-interconnection* $\mathcal{F}_l(M, \mathcal{K}_\infty)$ be defined [24] as,

$$T_{\mathrm{cl}} = \mathcal{F}_l(M, \mathcal{K}_\infty) = W_\Delta \mathcal{K}_\infty (\mathbb{I}_{N-1} - G_0 \mathcal{K}_\infty)^{-1}, \tag{12}$$

and let $\mathcal{A}_{\mathrm{cl}} \in \mathbb{R}^{n_{\mathrm{cl}} \times n_{\mathrm{cl}}}$, with $n_{\mathrm{cl}} = 2\left(n(N-1) + n_\Delta\right)$, denote the dynamic matrix associated with the closed-loop transfer function $T_{\mathrm{cl}}(s)$. The proposed $\mathcal{H}_\infty$-control design can be now stated in terms of the following convex optimisation problem:

$$\min_{\mathcal{K}_\infty \in \mathcal{RH}_\infty} \|\mathcal{F}_l(M, \mathcal{K}_\infty)\|_\infty = \gamma, \quad \text{s.t.} : \lambda(\mathcal{A}_{\mathrm{cl}}) \subset \mathcal{D}, \tag{13}$$

where $\mathcal{D}$ is a suitable selected LMI region[5]. Note that the control solution computed via (13) guarantees stability and well-posedness of the closed-loop structure of 11. Moreover, the following robust stabilisation condition

$$\|T_{\mathrm{cl}}\|_\infty = \|\mathcal{F}_l(M, \mathcal{K}_\infty)\|_\infty < \gamma, \tag{14}$$

is always satisfied, via the design objective (13).

[5] See [22] for a formal definition of LMI region.

*Remark* 10. The optimisation procedure stated in (13), explicitly considered to compute $\mathcal{K}_\infty$, can be efficiently solved using state-of-the-art LMI solvers, such as those described in, for instance, [25].

## 5. Case study

We now present a case study, addressing induced complete synchronization of a network of coupled FitzHugh-Nagumo oscillators. The FitzHugh-Nagumo model, commonly used to represent membrane voltage dynamics in neurons, is a simplified (two-dimensional) form of the well-known Hodgkin-Huxley neuron model (see [5]). To be specific, the FitzHugh-Nagumo system, characterising each $i$-th node of the network, can be written, in state-space, in terms of the following set of differential equations:

$$\Sigma_i : \begin{cases} \dot{x}_{i1} = \epsilon(x_{i2} - \delta x_{i1}), \\ \dot{x}_{i2} = -x_{i1} - x_{i2}(x_{i2} - 1)(x_{i2} - \xi) + u_i, \end{cases} \tag{15}$$

where $x_{i1}(t) \in \mathbb{R}$ is a recovery variable, $x_{i2}(t) \in \mathbb{R}$ represents the membrane voltage, and $u_i$ represents the (externally supplied) control input. Equation (15) is capable of exhibiting[6] structurally stable oscillations (*i.e.* limit cycles) by suitable tuning of the parameters $\{\xi, \epsilon, \delta\} \subset \mathbb{R}$.

With respect to the network topology, we consider four linearly coupled nodes, *i.e.* one leader and three slaves, where the corresponding coupling dynamics are of a linear nature. The interactions between nodes, arising from a 'ring' structure, are schematically depicted in Figure 3, and formally discussed in the following. In particular, the dynamics of the considered network can be described, in accordance to equation (3), by

$$A = \begin{bmatrix} -\epsilon\delta & \epsilon \\ -1 & -\xi \end{bmatrix}, \quad B = \begin{bmatrix} 0 \\ 1 \end{bmatrix}, \tag{16}$$

together with the set of mappings

$$\begin{aligned} g_{f_l}(x_l, \mathbf{x}) &= \tilde{g_f}(x_l) + \eta(x_{l2} - x_{22}) + \eta(x_{l2} - x_{42}), \\ g_{f_2}(x_l, \mathbf{x}) &= \tilde{g_f}(x_2) + \eta(x_{22} - x_{l2}) + \eta(x_{22} - x_{32}), \\ g_{f_3}(x_l, \mathbf{x}) &= \tilde{g_f}(x_3) + \eta(x_{32} - x_{22}) + \eta(x_{32} - x_{42}), \\ g_{f_4}(x_l, \mathbf{x}) &= \tilde{g_f}(x_4) + \eta(x_{42} - x_{l2}) + \eta(x_{42} - x_{32}), \end{aligned} \tag{17}$$

where $\tilde{g_f}(x_i) = -x_{i1}^3 + (1 + \xi)x_{i1}^2$, and $g(x_i) = 1$, for all $x_i(t) \in \mathbb{R}^2$. The constant value $\eta \in \mathbb{R}$ represents the so-called coupling *strength*. For this application case, the set of parameters $\{\xi, \epsilon, \delta\}$ has been selected such as (15) exhibits structurally stable oscillations, following [26]. Specifically, $\xi = -0.5$ and $\epsilon = \delta = 0.5$. The coupling strength is set to $\eta = 0.02$.

[6] A comprehensive assessment of the dynamics of (15) as a function of its parameters can be found in [26].

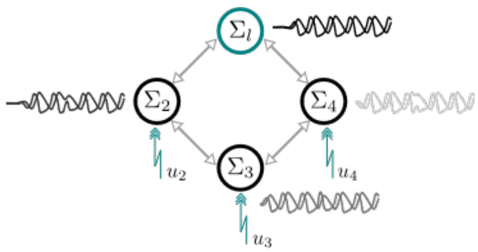


Figure 3: Schematic illustration of the network topology. The green circle indicates the leader node.

### 5.1. Controller design

The mappings described in (17) can be used to compute the feedback linearising strategy presented in Section 3, which directly facilitates the linearised structure presented in (8). The nominal model $G_0(s)$, used to design the stabilising control law $\mathbf{v}$ via $\mathcal{H}_\infty$-design, can be hence directly obtained from equation (16), *i.e.* in terms of the matrices $A$ and $B$ associated with each FitzHugh-Nagumo node. In addition, the family of models $\mathcal{G}$ is defined using the following multiplicative uncertainty weight,

$$W_\Delta(s) = \mathbb{I}_6 \otimes \frac{0.1s + 0.2}{\frac{2}{30}s + 1}. \tag{18}$$

Such a weight function is computed following Remark 9, assuming that the exact value of the parameter $\xi$ is not available, *i.e.* $\xi$ is uncertain. In particular, we consider $\pm 10\%$ of uncertainty about its nominal value $\xi_0 = -0.5$.

To successfully 'cover' the parametric uncertainty in $\xi$ via a family of models $\mathcal{G}$, a 20% of uncertainty (with respect to the nominal model $G_0$) is considered for $\omega < 2$ [rad/s], while a significantly larger uncertainty bound is required for higher values of $\omega$. The family $\mathcal{G}$ is shown in Figure 4, where the maximum singular value for any element in $\mathcal{G}$ is contained in the shadowed grey-area. Note that the magnitude corresponding with the nominal model $G_0$ is denoted using a dashed line.

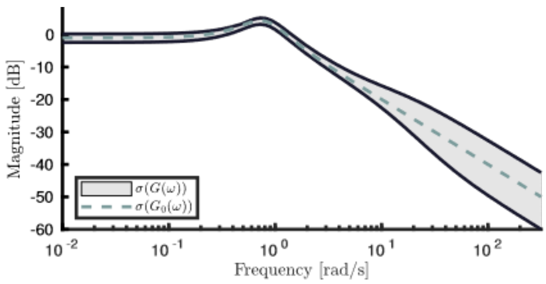


Figure 4: Maximum singular values for the family of models $\mathcal{G}$. The magnitude corresponding with the nominal model $G_0$ is denoted using a dashed line.

For this case study, the LMI region, considered to fully characterise the closed-loop dynamics, is defined as $\mathcal{D} = \{z \in \mathbb{C} : \Re(z) \in [-100, -2]\}$. The stabilising controller $\mathcal{K}_\infty$ is then directly computed via the optimisation problem (13), obtaining a performance level $\gamma = 0.4 < 1$. Figure 5 presents the maximum singular value of $T_{\text{cl}}$, and the corresponding performance $\gamma$, using solid and dotted lines, respectively. Note that the closed-loop behaviour satisfies both the design objective $\bar{\sigma}(T_{\text{cl}}(\jmath\omega)) < \gamma$, and the well-known stability condition $\|\Delta(s)\|_\infty < \|W_\Delta(s)\|_\infty < \frac{1}{\gamma}$.

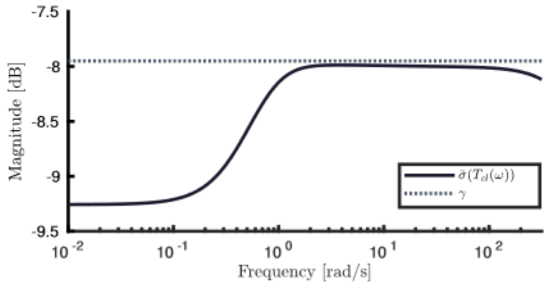


Figure 5: Maximum singular value of the closed-loop transfer function $T_{\text{cl}}$ (solid line) and control performance $\gamma$ (dotted line).

### 5.2. Controller results

Considering the control design procedure detailed in Section 5.1, the time-traces of the controlled complex network are shown in Figure 6, switching from open- to closed-loop when $t \approx 35$ [s]. Note that, different sets of state-trajectories can be appreciated in the open-loop regime, complete synchronization is not achieved until after the proposed control strategy is applied. In particular, at $t \approx 35$ [s], the control loop is closed, and the state-vector $x_i(t) \in \mathbb{R}^2$ of each slave node (dotted) synchronises with the state-vector of the master node (solid) by virtue of the externally applied control force, *i.e.* complete synchronization is successfully induced by the controller.

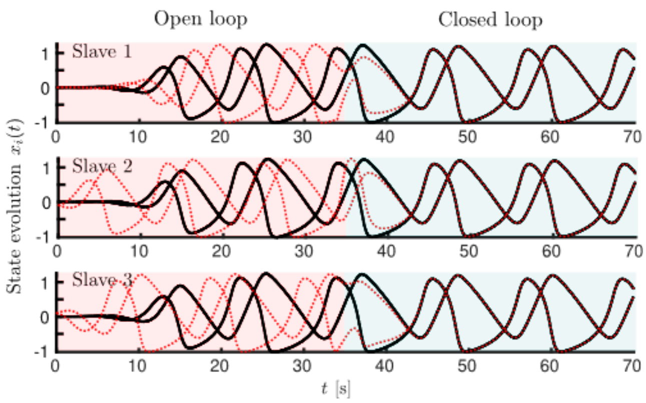


Figure 6: Time-traces of the state-vector of each slave (node 1 to 3, dotted), and leader node (solid). After the proposed controller is applied ($t \approx 35$ [s]), complete synchronization is successfully achieved.

Finally, and to briefly showcase the robustness features of the proposed control technique, Figure 7 illustrates the time-traces corresponding with the state-vector of the error system $e_i(t) \in \mathbb{R}^2$ for each node, both when the nominal model is considered for simulation (dotted), *i.e.* the controller achieves nominal performance, and when the model used for simulation features a $-10\%$ of uncertainty

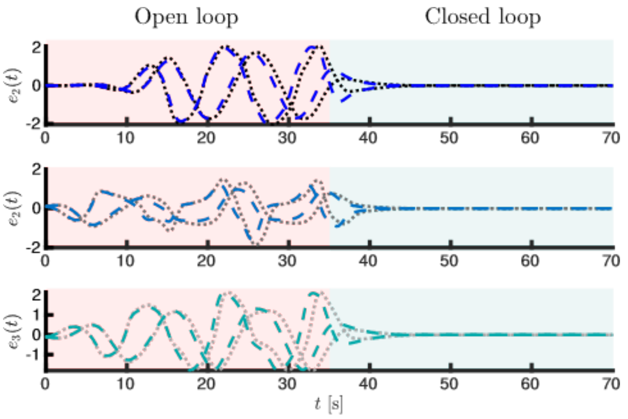


Figure 7: Time-traces of the state-vector of each synchronization error system when: no uncertainty is present in the simulation model (dotted); the parameter $\xi$ features a -10% of uncertainty in the simulation model, *i.e.* $\xi = 0.9\xi_0$ (dashed).

in $\xi$, *i.e.* $\xi = 0.9\xi_0$. It can be readily appreciated that, after the proposed controller is applied, the error dynamics are stable even under the presence of parametric uncertainty (and, hence, an inexact linearisation procedure), facilitated through the robust control design procedure.

## 6. Conclusions

This short communication presents a framework to control complete synchronization for a general class of network-coupled nonlinear oscillators, *i.e.* to induce synchronization by means of a suitable user-supplied *external control force*, under mild assumptions. To this end, we propose a multiple-input multiple-output feedback decoupling linearisation algorithm, used to express the closed-loop synchronization error dynamics in terms of a linear operator. Motivated by the fact that feedback linearisation relies on precise knowledge of the network dynamics, which might not be available in realistic scenarios, we propose a robust control scheme based on $\mathcal{H}_\infty$-control synthesis and pole placement, capable of achieving complete synchronization even in the presence of modelling uncertainty. We explicitly illustrate the capabilities of the technique for a complex network of FitzHugh-Nagumo neurons.

### Acknowledgment

This material is based upon works supported by Science Foundation Ireland under Grant no. 13/IA/1886.

## References

[1] S. H. Strogatz, Exploring complex networks, Nature 410 (6825) (2001) 268–276.

[2] A. Pikovsky, J. Kurths, M. Rosenblum, J. Kurths, Synchronization: a universal concept in nonlinear sciences, Vol. 12, Cambridge University Press, 2003.

[3] P. S. Skardal, A. Arenas, Control of coupled oscillator networks with application to microgrid technologies, Science advances 1 (7) (2015) e1500339.

[4] N. Faedo, G. Scarciotti, A. Astolfi, J. V. Ringwood, Moment-based constrained optimal control of an array of wave energy converters, in: 2019 American Control Conference (ACC), IEEE, 2019, pp. 4797–4802.

[5] G. B. Ermentrout, D. H. Terman, Mathematical foundations of neuroscience, Vol. 35, Springer Science & Business Media, 2010.

[6] J. V. Ringwood, S. C. Malpas, Slow oscillations in blood pressure via a nonlinear feedback model, American Journal of Physiology-Regulatory, Integrative and Comparative Physiology 280 (4) (2001) R1105–R1115.

[7] L. M. Pecora, T. L. Carroll, Synchronization in chaotic systems, Physical review letters 64 (8) (1990) 821.

[8] V. N. Belykh, I. V. Belykh, M. Hasler, Connection graph stability method for synchronized coupled chaotic systems, Physica D: nonlinear phenomena 195 (1-2) (2004) 159–187.

[9] V. N. Belykh, E. V. Pankratova, E. Mosekilde, Dynamics and synchronization of noise perturbed ensembles of periodically activated neuron cells, International Journal of Bifurcation and Chaos 18 (09) (2008) 2807–2815.

[10] L. M. Pecora, T. L. Carroll, Master stability functions for synchronized coupled systems, Physical review letters 80 (10) (1998) 2109.

[11] J. Pastor, R. G. de Sola, G. J. Ortega, Hyper-synchronization, de-synchronization, synchronization and seizures, in: Epilepsy, IntechOpen, Rijeka, 2012, Ch. 6.

[12] Y.-Q. Che, J. Wang, S.-S. Zhou, B. Deng, Robust synchronization control of coupled chaotic neurons under external electrical stimulation, Chaos, Solitons & Fractals 40 (3) (2009) 1333–1342.

[13] J. Gao, Y.-Y. Liu, R. M. D'souza, A.-L. Barabási, Target control of complex networks, Nature communications 5 (1) (2014) 1–8.

[14] W. Jiang, D. Bin, K. Tsang, Chaotic synchronization of neurons coupled with gap junction under external electrical stimulation, Chaos, Solitons & Fractals 22 (2) (2004) 469–476.

[15] H. Yu, J. Wang, B. Deng, X. Wei, Y. Che, Y. Wong, W. Chan, K. Tsang, Adaptive backstepping sliding mode control for chaos synchronization of two coupled neurons in the external electrical stimulation, Communications in Nonlinear Science and Numerical Simulation 17 (3) (2012) 1344–1354.

[16] D. López-Mancilla, G. López-Cahuich, C. Posadas-Castillo, C. Castañeda, J. García-López, J. Vázquez-Gutiérrez, E. Tlelo-Cuautle, Synchronization of complex networks of identical and nonidentical chaotic systems via model-matching control, Plos one 14 (5) (2019) e0216349.

[17] J. Nagumo, S. Arimoto, S. Yoshizawa, An active pulse transmission line simulating nerve axon, Proceedings of the IRE 50 (10) (1962) 2061–2070.

[18] G. Rigatos, Advanced models of neural networks, in: Nonlinear dynamics and stochasticity in biological neurons, Springer, 2013.

[19] H. K. Khalil, Nonlinear Systems, Prentice-Hall, New Jersey, 1996.

[20] H. Su, X. Wang, Pinning control of complex networked systems: Synchronization, consensus and flocking of networked systems via pinning, Springer Science & Business Media, 2013.

[21] P. Gahinet, P. Apkarian, A linear matrix inequality approach to $\mathcal{H}_\infty$ control, International Journal of Robust and Nonlinear Control 4 (1994) 421–448.

[22] M. Chilali, P. Gahinet, $\mathcal{H}_\infty$ control design with pole placement constraints: An LMI approach, IEEE Transactions on Automatic Control 41 (3) (1996) 358–367.

[23] G. E. Dullerud, F. Paganini, A course in robust control theory: a convex approach, Vol. 36, Springer Science & Business Media, 2013.

[24] R. S. Sánchez Peña, M. Sznaier, Robust Systems Theory and Applications, John Wiley & Sons, Inc., 1998.

[25] J. F. Sturm, Using SeDuMi 1.02, a MATLAB toolbox for optimization over symmetric cones, Optimization methods and software 11 (1-4) (1999) 625–653.

[26] M. Ringkvist, Y. Zhou, On existence and nonexistence of limit cycles for fitzhugh-nagumo class models, in: New Directions and Applications in Control Theory, Springer, 2005, pp. 337–351.